The functions of ocu-miR-205 in regulating hair follicle development of Rex rabbits

Gongyan Liu
Shandong Agricultural University
Shu Li
Shandong Agricultural University
Hongli Liu
Shandong Agricultural University
Yanli Zhu
Shandong Agricultural University
Liya Bai
Shandong Academy of Agricultural Sciences
Haitao Sun
Shandong Academy of Agricultural Sciences
Shuxia Gao
Shandong Academy of Agricultural Sciences
Wenxue Jiang
Shandong Academy of Agricultural Sciences
Fuchang Li (chlf@sdau.edu.cn)
Shandong Agricultural University https://orcid.org/0000-0002-5670-8038

Research article

Keywords: Rex rabbit, Dermal papilla cell, ocu-miR-205, Hair follicle density

Posted Date: August 31st, 2019

DOI: https://doi.org/10.21203/rs.2.13789/v1

Version of Record: A version of this preprint was published at BMC Developmental Biology on April 22nd, 2020. See the published version at https://doi.org/10.1186/s12861-020-00213-5.

Abstract

Background: Hair follicles is an appendage from the vertebrate skin epithelium, and arise from the embryonic ectoderm andregenerate cyclically during adult life. Dermal papilla cells (DPCs) is the key dermal component of the hair follicle that directly regulates hair follicle development, growth and regeneration. Recent studies have reported that miRNA plays an important role in regulating hair follicle morphogenesis, proliferation, differentiation and apoptosis of hair follicle stem cells. Results: The miRNAs expression profile of the DPCs from different hair density Rex rabbits shown that 240 differentially expressed of miRNAs were screened (log 2 (HD/LD)>1.00 and Q-value≤0.001). Among them, the expression of ocu-miR-205-5p in low hair densities DPCs was higher than that in high hair densities, and it is highly expressed in the skin tissue of Rex rabbits (P <0.05). ocu-miR-205 could increase cell proliferation and cell apoptosis ratio, change cell cycle process (P <0.05), affect the genes expression of PI3K/Akt, Wnt, Notch and BMP signaling pathways in DPCs and skin tissue of Rex rabbits, inhibit the protein phosphorylation level of CTNNB1, GSK-3β and the protein expression level of noggin (NOG), promote Akt phosphorylation level (P <0.05). There was no significant change in primary follicle density (P >0.05), but the secondary follicle density and total follicle density (P <0.05) were changed after ocu-miR-205-5p interfered expression, and secondary/primary ratio (S/P) in ocu-miR-205-5p interfered expression group increased at 14 days after injection (P <0.05). Conclusion: ocu-miR-205 could promote the apoptosis of DPCs, affect PI3K/Akt, Wnt, Notch and BMP signaling pathways genes and proteins expression in DPCs and skin of Rex rabbits, promote the transformation of hair follicles from growth phase to regression and resting phase, and affect hair density of Rex rabbits.

Background

Rex rabbits are famous for fur production, and the fur is short, fine, dense, smooth and has important economic values [1]. The most important indicator for evaluating the quality of Rex rabbit fur is the density of hair follicle [2]. In recent years, how to improve the hair follicle density of Rex rabbits has become the most important concern in rabbit production. Hair follicles is an appendage from the vertebrate skin epithelium, and arise from the embryonic ectoderm andregenerate cyclically during adult life [3]. In the process of hair follicles formation and differentiation, involves at least 20 different cells [4], including dermal papilla, hair matrix, inner root sheath, outer root sheath, and different signaling pathways such as Wnt, Notch, Bone morphogenetic protein (BMP), Fibroblast growth factor (FGF), and so on [5-9]. Phosphatidylinositol 3'-kinase (PI3K) can preferentially phosphorylate PIP2 to produce PIP3, and PIP3 is an important second messenger in cells, which can activate downstream Akt, plays an important role in proliferation and apoptosis of hair follicle cells. Wnt signaling pathway can regulates epithelial morphogenesis, hair follicle development and cell differentiation. The PI3K/Akt signaling pathway can inhibit the phosphorylation of β-catenin by phosphorylating Glycogen synthase kinase 3β (GSK-3β) and activate Wnt signaling pathway[5]. Dickkopf relative protein 1 (DKK1) can inhibit Wnt signaling pathway by inhibiting phosphorylation of β-catenin and induce hair follicle regression [10]. When Notch receptor binds to ligand, it can activate hair follicle stem cells and then promote hair follicle from resting stage to growing stage[6]. BMP signaling pathway is involved in embryonic skin appendage organ morphogenesis and postnatal hair follicle growth[7]. BMP2 and BMP4 genes inhibit hair follicle development and are associated with maintaining hair follicle rest[8]. Noggin (NOG) acts as an inhibitor of BMP signaling pathway, and its abnormal expression leads to follicular enlargement [7]. Notch signaling pathway interacts with BMP signaling pathway, and BMP signaling pathway can inhibit Wnt signaling pathway by regulating β-catenin [6]. Dermal papilla (DP) comprises of a group of specialized mesenchymal cells that are embedded in the hair bulb at the base of the follicle, is considered the control center of hair follicle growth and hair cycle. Dermal papilla cells (DPCs) govern hair follicle development and growth, and instruct the surrounding matrix cells to proliferate, move upward and differentiate into the outgrowing hair shaft and the channel called inner root sheath [11]. Moreover, the number of DPCs also specifies hair size, shape and cycling [12]. Signal exchange between dermal papilla cells and hair follicle stem cells at telophase is the key to initiating the next hair follicle cycle [13].

MicroRNAs (miRNAs) are the small (~22 nucleotides long), non-coding RNAs that have been proposed to play important roles in diverse biological processes [14], such as organ development, cell proliferation, tumorigenesis, fat metabolism,

behavior and embryogenesis [15-19]. Recent studies have reported that miRNA plays an important role in regulating hair follicle morphogenesis, proliferation, differentiation and apoptosis of hair follicle stem cells in mice, rat, goat and sheep [20-22]. miR-214 inhibits hair follicle growth and development by regulating regulatory factors such as β-catenin and lymphoid enhancer-binding factor 1 (Lef-1) in Wnt signaling pathway [23]. After overexpression of DKK1 in transgenic mice, the expression of miR-200b and miR-196a in epidermis decreased significantly, possibly through potential target genes acting on Wnt signals [24]. miR-let-7b promotes alpaca hair growth by inhibiting the transcription of transforming growth factor β receptor 1 (TGFβR1) [25]. BMP4 negatively regulated the expression of miR-21, and also confirmed that miR-21 negatively regulated the expression of BMP-dependent tumor suppressor genes Pten, Pdcd4, Timp3 and Tpm1 [26]. miR-31 can regulate hair follicle development and hair growth in mice through BMP and Wnt signaling pathways [20]. miR-205 is a highly conserved microRNA and shares a similar expression pattern with miR-200 family [27], is one of the most abundant skin miRNAs expressed in epidermis [28, 29], it has an essential role in promoting neonatal expansion of skin stem cells during early development by modulating the PI3K pathway [30].

In order to improving the fur quality of Rex rabbits, we isolated the DPCs from Rex rabbits skin, and analyzed the miRNAs expression profile of the DPCs from different hair density Rex rabbits. Among them, ocu-miR-205 is one of the most highly expressed miRNAs in skin. We demonstrate the function of ocu-miR-205 in hair follicle dopmevelent.

Methods

Animals

The Rex rabbits in this study were purchase from Taishan Rabbit Farm (Shandong, China). Selected animals were electrically stunned (120 V, pulsed direct current, 50 Hz for 5 sec) and killed by carotid artery bloodletting and slaughtering before skin harvesting in experimental rabbits.

Isolation and culture of DPCs from Rex rabbits

Small skin pieces from 30-day-old Rex rabbits were rinsed with sterile phosphate buffer saline (PBS; Solarbio, China) containing 100 U/mL penicillin and 0.1 mg/mL streptomycin, disinfected with iodine and destained with 75% ethanol, then cut into 20 mm*50 mm strips before digesting with 0.25 mg/ml Dispase II (Sigma, Cat. D4693, USA) overnight at 4 °C and with an additional 30 min incubation at 37 °C on the following day. The tissues were then minced with ophthalmological scissors and digested with 0.1 mg/ ml Collagenase D (Sigma, Cat. C2674, USA) for 6 h at 37 °C when dissociation of DPs from liquid fats was observed by microscopy (Nikon Ts2FL, Japan) [52]. Subsequently, DPs were purified by a series of washing with PBS till the supernatant was completely clear, and filtered with a 75 mM filter to remove single cells. Following purification, DPs were trypsinized to obtain single cells which were then cultured in dulbecco's modified eagle medium (DMEM; Gibco, USA) containing 10% fetal bovine serum (FBS; Gibco, USA) at 37°C in a humidified atmosphere of 95% air and 5% CO2.

Construction of the small RNA libraries, sequencing analysis, miRNAs identification and prediction of new miRNAs in DPCs

Small RNA fragments measuring 18–30 nt were isolated and puri-fied from the total RNA using 15% denaturing polyacrylamide gel electrophoresis (PAGE). Subsequently, 3' and 5' RNA adaptors were ligated to the RNA pool using T4 RNA ligase, and the samples were used as templates for cDNA synthesis. The cDNAs were amplified using the appropriate number of PCR cycles needed to produce the sequencing libraries, which were subsequently subjected to the proprietary Solexa sequencing by synthesis method using the BGISEQ-500 platform at Shenzhen Huada Biotech Co., Ltd. [53, 54] (Shenzhen, China).

The raw reads produced by the BGISEQ-500 sequencing were filtered to remove low quality reads, and those that passed the quality filter were trimmed to remove the 5' and 3' adaptor sequences. Similarly, the reads with a poly (A) sequences were removed. The length distribution of the clean reads was calculated. The remaining reads were analyzed by BLAST against

Bowtie-1.0.0 software, Rfam [55] and Repbase to discard messenger RNA (mRNA), ribosomal RNA (rRNA), transfer RNA (tRNA), small nuclear ribonucleic acid (snRNA), small nucleolar RNA (snoRNA) and repeat sequences. The remaining sequences were used for miRNA identification in comparison with the mature miRNAs and pre-miRNAs from *Oryctolagus cuniculus* listed in miRBase 21.0 [56], with permission of one mismatch. Later on, the miRDeep 2 software [57] was used to predict the novel miRNAs by exploring the secondary structure, Dicer cleavage site and minimum free energy of the unannotated small RNA tags that could be mapped to the *Oryctolagus cuniculus* genome. The remaining sequences after conserved miRNAs identification were aligned to the *Oryctolagus cuniculus* genome in order to identify new *Oryctolagus cuniculus* miRNAs. Certain target sequences around the small RNA were used to explore the secondary structure and folding energy (218 kcal/mol).

Transcript per million (TPM) was used to standardize the expression level of small RNA [58], which could avoid the impact of different sequencing quantities on quantitative accuracy. Based on the assumption that RNA sequencing is a random process, each sequence is uniformly random from its own sample [59], it can be assumed that the expression of each transcript follows a binomial distribution. Using the above model, DEGseq calculated differential expression based on MA-plot [60, 61]. Assuming that C1 and C2 are the total Reads on the comparison of two samples, they obey binomial distribution. Define Textit {M}= $\log_2$ C1 - $\log_2$ C2, A= ($\log_2$ C1 + $\log_2$ C2) /2. It can be proved that under the condition of random sampling, the distribution of M obeys A=a and approximates normal distribution. The P-value of each miRNA was corrected by multiple hypothesis tests using Q-value. The difference of coincidence was more than twice and the value of Q-value was less than or equal to 0.001, so it was considered that there was significant difference in the expression of miRNAs.

To better explore the potential function of the miRNAs having significantly different expression between the different hair density Rex rabbit, the miRNAs were aligned to the EST unigenes of *Oryctolagus cuniculus* to predict the target genes by miRanda algorithm [62]. Enrichment analysis of the predicted target genes was conducted with GO and KEGG pathway [63].

Construction and identification of ocu-miR-205 over expression and interfering expression adenovirus vector

HBAD-GFP (HANBIO Adenovirus-Green flourecent protein; Empty vector), HBAD-ocu-miR-205-GFP (Over expression), HBAD-ocu-miR-205-5p-sponge-GFP (Interference expression) adenovirus were synthesized and constructed by Hanheng Biotechnology Co., Ltd. (Shanghai, China). The infective titers of HBAD-GFP, HBAD-ocu-miR-205-GFP and HBAD-ocu-miR-205-5p-sponge-GFP were $1.26*10^{10}$ PFU/mL, $1.58*10^{10}$ PFU/mL and $1.26*10^{10}$ PFU/mL, respectively.

The third generation dermal papilla cells in good growth condition were inoculated into a disposable 6-well plate. The cell concentration was about $1.0*10^5$ count/mL. Before infection, the virus was diluted by 10-fold gradient. Generally, the MOI (Multiplicity of infection) was controlled in the range of 10-1000. HBAD-GFP, HBAD-ocu-miR-205-GFP and HBAD-ocu-miR-205-GFP were transfected into Rex rabbit dermal papilla cells as MOI 200, respectively, and negative control was set up in normal culture.

The purified adenovirus was injected into the skin of each Rex rabbits by microinjector 50 μL according to the number of $5.0*10^8$ ~ $1.0 * 10^9$ virus particles per Rex Rabbit after shaving the middle part of the back of 100 3-month-old Rex rabbits with similar body weight and good health. 24 hours after transfection, random selection one Rex rabbit was slaughtered and frozen sections were made from the local injected skin of each group. The adenovirus transfected skin was observed under a positive fluorescence microscope (Nikon ECLIPSE 80i, Japan).

Proliferation, cell cycle and apoptosis determination of DPCs

DPCs were plated in a 96-well plate at a density of 10^4 count/well and cultured in basal medium for 24 h, and then followed by the indicated treatment. Thiazolyl blue tetrazolium bromide (MTT, Solarbio) was added to each pore at 20 μL 5 g/L for 4 hours, and dimethyl sulfoxide (DMSO, Solarbio, China) was added to each pore at 37 °C. Optical density (OD) value was read at 490 nm by enzyme labeling instrument (BioTek Elx-808, USA) after 10 minutes of oscillation. Within a certain cell number range, the amount of MTT crystallization is proportional to the number of cells. According to the measured OD value, we can

judge the number of living cells. The larger the OD value, the stronger the cell proliferation activity. For flow cytometry analysis, the DPCs were treatment followed by the indicated treatmented. The cells were digestion by trypsin and fixed in 70% cold ethanol for at least 18 h, centrifuged at 500 g for 5 min, dropped the supernate and added 0.5 mL propidium iodide (PI; BD Biosciences, Cat: 550825) for incubating 15 min at 37 °C in dark. The cells were then analyzed by flow cytometry (BD Accuri C6, BD). And the results were analyzed with the ModFit LT 5.0 software.

The third generation DPCs were inoculated with 10^4 count/mL on a disposable 6-well plate, with 2 mL cell suspension per hole. After 24 hours adherence, the culture medium was removed. After treatment and culture for a certain time, the cells were digested with trypsin digestion solution without EDTA (Solarbio, China). Centrifuged and collected into a 1.5 mL centrifugal tube. PBS washed the cells. After centrifugation, 500 μL 10X Annexin V Binding Buffer re-suspended cells were added, followed by F-acting. FITC Annexin V and Proidium Iodide Staining Solution were incubated at 4 °C for 15 minutes and then tested on the computer. The percentage of early apoptotic cells (Q4), later apoptotic cells (Q2) and total apoptotic cells (Q2 + Q4) in each sample was counted.

Total RNA extraction and Real-time PCR analysis

Total RNA in tissues or cells were extracted with RNAiso reagent (TaKaRa, Japan), following the manufacturer's instructions. The integrity and quality of the total RNA were evaluated using a 2100 Bioanalyzer RNA Nano chip device (Agilent, Santa Clara, CA, USA) and agarose gel electrophoresis respectively, and the concentration was measured with a ND-1000 spectrophotometer (NanoDrop, Wilmington, DE).

For mRNA quantitative RT-PCR, 1 μg of total RNA of was used to synthesize cDNA using a Transcriptor First Strand cDNA Synthesis Kit (Roche Diagnostics GmbH Mannheim, Germany), mRNA quantitative RT-PCR was performed to determine the expression levels of target genes and glyceraldehyde-3-phosphate dehydrogenase (GAPDH) was used as a reference gene. All quantitative PCR primers (Additional file 11) were designed by Primer Premier 5 software and synthesised by SANGON Biological Engineering Co., Ltd (Shanghai, China). PCR amplification was performed using Fast Start Universal SYBR Green Master (Roche Diagnostics GmbH Mannheim, Germany). The volume of each PCR reaction was 20 μL, including 2 μL cDNA, 10 μL SYBR Premix Ex Taq^{TM} (2×), 0.5 μL PCR Forward Primer (10 μM), 0.5 μL PCR Reverse Primer (10 μM), 0.4 μL ROX Reference Dye II (50×) and 6.6 μL ddH_2O. The number of cycles set for the linear amplification of the cDNA was 40. All samples were run in duplicate, and the standard curves were generated using pooled cDNA from the samples being assayed.

For miRNA quantitative RT-PCR, 1 μg of total RNA was reversely transcribed with Bulge-Loop miRNA-specific reverse transcription-primers (RiboBio, China) and quantitative PCR reactions were using Fast Start Universal SYBR Green Master (Roche Diagnostics GmbH Mannheim, Germany), and Bulge-Loop primers (RiboBio, China) on the 7500 Fast System 1.4 system with small nuclear RNA U6 as the normalisation control. The volume of each PCR reaction was 20 μL, including 2 μL cDNA, 10 μL SYBR Green Master (2X), 0.8 μL Bulge-Loop^{TM} miRNA Forward Prime (5μM), 0.8 μL Bulge-Loop^{TM} Reverse Prime (5μM), 0.4 μL ROX Reference Dye II (50×) and 6.0 μL ddH_2O. System under the following conditions: 10 min template denaturation at 95 °C, followed by 40 cycles of 95 °C for 2 s, 60 °C for 20 s, and 70 °C for 10 s followed by the melting curve (70 °C-95 °C). Melting curves for each sample were analyzed after each run to check the specificity of amplifications. Three biological replicates with three technical replications were conducted for each qRT-PCR. The relative expression level of mRNA and miRNA was calculated according to the arithmetic formula $2^{-\triangle\triangle Ct}$ [65].

Western immunoblotting.

Tissues or cells were lysed in RIPA buffer on ice for 30 min. The supernatant was centrifuged for 30 min at 12,000 g and 4 °C, and protein concentrations were determined using a BCA Protein Assay Kit (Kangwei, China), The extracted proteins (50 ng/sample) were solubilized in 40 millimole SDS-loading buffer (Solarbio, China) and then resolved by electrophoresis (Bio-Rad, Richmond, USA) and 12.5% SDS-PAGE prior to being transferred electrophoretically to a polyvinylidene fluoride (PVDF) membranes (Millipore, Billerica, USA). The standard markers for protein molecular masses were purchased from Thermo

(USA). The membranes were blocked with 5% skimmed milk in PBS (Solarbio, China) at 4 °C overnight and incubated with primary antibodies (Tubulin AT819, Beyotime, China; Phospho-CTNNB1-S552 pAb, Abcam, US; Phospho-GSK3B-S9 pAb, Abcam, US; Phospho-AKT1-S473 pAb, Abcam, US; NOG Polyclonal Antibody, Abcam, US). The membranes were then rinsed in Tris Buffered Saline Tween (TBST; Solarbio, China), and subjected to detection with 1:3000 diluted horse radish peroxidase (HRP)-conjugated goat anti-mouse IgG antibody (Beyotime, China) at 37 °C for 1 h. Proteins were visualized using BeyoECL reagents (Beyotime, China). The intensity of the bands was quantified by a Pro Plus 6.0 Biological Image Analysis System Phospho-CTNNB1, Phospho-GSK3B, Phospho-AKT1 and NOG were normalized to the internal control beta-tubulin, and the relative expression levels were calculated.

Statistical analysis

All the data were analyzed with SAS software (SAS version 8e; SAS Institute, Cary. NC, USA). A one-way ANOVA model was used to evaluate the means among various groups. The data were shown as means and R-MSE. $P < 0.05$ was regarded as statistically significant.

Results

DPCs show miRNA expression complexity

To evaluate the varieties of miRNAs in DPCs from lower and higher denisty hair follicle of the 30-day old Rex rabbits (Additional file 1), RNA samples with high integrity and qualified quality (Additional file 2), high throughput small RNA sequencing was carried out using BGISEQ-500 platform on small RNA libraries. We obtained 37930744, 39442011, 40965907, 38502653, 40622117 and 41149163 clean reads in total from the six samples (Additional file 3), and the majority of clean reads have a length of 23 nucleotides (Additional file 4), which was consistent with the size of mammalian miRNAs. Comparing with known small RNA databases, more than 90 % of the clean reads in six libraries can be matched, which were 91.91 %, 91.05 %, 92.46 %, 92.77 %, 90.13 %, and 91.61 %, respectively (Additional file 5). The results of the small RNA classification commentary shown that miRNAs accounted for 80.80 %, 82.50 %, 81.60 %, 85.80 %, 76.50 %, and 81.80 %, respectively (Additional file 6). The base Q20 of filtered data was more than 90% and Q30 was more than 80%, the quality of the data was reliable. Additional file 7 and Additional file 8 was the quantity and quality distribution maps of the base of each sample, respectively.

Through differentially expressed genes screen (DEGs), 240 differentially expressed of miRNAs were screened ($\log_2$(HD/LD)| >1.00 and Q-value≤0.001; Fig. 1a; Additional file 9), including 122 miRNAs for up regulate and 118 miRNAs for down regulate (Fig. 1b). The annotation of the targeted gene of differentially expressed miRNAs was performed using Gene Ontology (GO) enrichment and Kyoto Encyclopedia of Genes and Genomes (KEGG) pathway analysis. A total of 205,661 target genes were enriched into GO terms (Fig. 1c), specific GO terms of the target genes were mainly involved in biological process (BP), cellular component (CC) and molecular function (MF). Directed Acyclic Graph (DAG) of GO enrichment of BP, CC and MF was shown in Additional file 10. Following GO analysis, the target genes were also uploaded into the KEGG database to identify the pathway that were actively regulated by miRNAs in dermal papilla cells. The results shown that a total of 325 pathways were predicted. Top enrichment pathways was Wnt signaling pathway, Notch signaling pathway, et al. (Fig. 1d).

The expression of ocu-miR-205

Among them, the structure of ocu-miR-205 was shown in Fig. 2a, ocu-miR-205 in DPCs of Rex rabbits with different densities was different ($\log_2$(HD/LD)|>1.00 and Q-value≤0.001; Fig. 2b), and was low expressed in DPCs of Rex rabbits with high hair density (HD) and high expressed in DPCs of Rex rabbits with low hair density (LD). Quantitative fluorescence PCR results also confirmed the accuracy of ocu-miR-205-5p sequencing results (Fig. 2c). Further, the expression of ocu-miR-205-5p in

different tissues of Rex rabbits was different (P<0.05), the expression in skin tissue was higher than that in stomach, intestine, spleen, liver, heart, lung, kidney, muscle and fat (P<0.05; Fig. 2d), has tissue specificity.

Effects of ocu-miR-205 on DPCs of Rex rabbits

HBAD-GFP, HBAD-ocu-miR-205-GFP, HBAD-ocu-miR-205-5p-sponge-GFP were constructed and transfect DPCs as multiplicity of infection (MOI) 200. Cell proliferation, cell cycle, cell apoptosis, ocu-miR-205-5p and hair follicle development-related gene and protein changes were detected 48 hours after transfection. The results shown that constructed adenovirus could successfully transfect DPCs (Fig. 3a), and the expression of ocu-miR-205-5p increased significantly after overexpression, while the expression of ocu-miR-205-5p decreased significantly after interference (P<0.05; Fig. 3b). ocu-miR-205 could increase cell proliferation and cell apoptosis ratio, change cell cycle process (P<0.05; Table 1). ocu-miR-205 could inhibit the gene expression of Inppl1, Frk and Phlda3 in PI3K/Akt signaling pathway (P<0.05). ocu-miR-205 could promote DKK1 and inhibit Wnt10b, CTNNB1 and GSK-3β gene expression in Wnt signaling pathway (P<0.05). Notch1, Jagged1, Hes1 and Hes5 expression in Notch signaling pathway were suppressed by ocu-miR-205 (P<0.05), and BMP2, BMP4 and TGF-β1 expression in BMP signaling pathway were promoted (P<0.05; Table 2). ocu-miR-205 could inhibit the protein phosphorylation level of CTNNB1, GSK-3β and the protein expression level of noggin (NOG), promote Akt phosphorylation level (P<0.05; Fig. 4).

Effects of ocu-miR-205 on skin tissue of Rex rabbits

One hundred 3-month-old Rex rabbits with similar body weight were randomly divided into 4 groups. After local shaving of the back skin, HBAD-GFP, HBAD-ocu-miR-205-GFP and ocu-miR-205-5p-sponge-GFP 50 μL per rabbit were injected intradermally. 24 hours after transfection, random selection one Rex rabbit of each group was slaughtered and frozen sections were made from the local injected skin to observation the transfection, 8 Rex rabbits were randomly selected from each group 7 days, 14 days and 21 days after transfection. After slaughter, the injected skin was collected and placed in freezing tube and 4% polyformaldehyde stationary solution. The frozen samples were used to detect the changes of ocu-miR-205-5p and hair follicle development-related gene and proteins. The fixed samples were used to make paraffin sections and the hair density was counted after HE staining. The results shown that constructed adenovirus could successfully transfect the skin and hair follicles of Rex rabbits (Fig. 5a), and the expression of ocu-miR-205-5p increased significantly after overexpression, while the expression of ocu-miR-205-5p decreased significantly after interference (P<0.05; Fig. 5b). After transfection 14 days, ocu-miR-205 could significantly affect gene expression in PI3K/Akt, Wnt, Notch and BMP signaling pathways (P<0.05; Table 3). ocu-miR-205 could significantly affect the protein phosphorylation level of CTNNB1, GSK-3β, Akt and the expression protein level of NOG (P<0.05; Fig. 6). There was no significant change in primary follicle density (P>0.05), but the secondary follicle density and total follicle density (P<0.05) were changed after ocu-miR-205-5p interfered expression, and secondary/primary ratio (S/P) in ocu-miR-205-5p interfered expression group increased at 14 days after injection (P<0.05; Table 4).

Discussion

miRNAs are considered as the key regulators of gene expression at the post-transcriptional level and to perform a variety of significant functions within cells such as regulation of growth, metabolism, development and cell differentiation [31-33]. DPCs of various origins are able to induce de novo formation of hair follicle structure in both follicular and afollicular epidermis [34-37], implying a potential therapeutic application of DPCs in the treatment of alopecia. miR-205 is one abundant keratinocyte-specific miRNA in the epidermis [37, 38]. It has an essential role in promoting neonatal expansion of skin stem cells during early development by modulating the PI3K/Akt pathway [39]. PI3K/Akt signaling pathway can inhibit the phosphorylation of β-catenin by phosphorylating GSK-3β and activate Wnt signaling pathway [5]. DKK1 can inhibit Wnt signaling pathway by inhibiting phosphorylation of β-catenin and induce hair follicle regression [10]. When Notch receptor binds to ligand, it can activate hair follicle stem cells and then promote hair follicle from resting stage to growing stage [6]. BMP signaling pathway is involved in embryonic skin appendage organ morphogenesis and postnatal hair follicle growth [7]. BMP2 and BMP4 genes inhibit hair follicle development and are associated with maintaining hair follicle rest [8]. Noggin

acts as an inhibitor of BMP signaling pathway, and its abnormal expression leads to follicular enlargement [40]. Notch signaling pathway interacts with BMP signaling pathway, and BMP signaling pathway can inhibit Wnt signaling pathway by regulating β-catenin [6].

Although the effects of miR-205 in keratinocyte migration have been investigated in some in vitro models [41, 42]. In vitro studies using both primary human epidermalb keratinocytes and corneal epithelial keratinocytes indicate that miR-205 can promote keratinocyte migration via targeting the lipid phosphatase SHIP2 and KIR4.1 respectively [41, 42]. While, as to role of miR-205 in cell migration, different studies have reported conflicting results in different models. Some indicate that miR-205 can promote migration [43, 44], however, others show opposite results [45-50]. In this study, we found the expression of ocu-miR-205-5p in low hair densities DPCs was significantly higher than that in high hair densities. Ocu-miR-205 could induce G0/G1 arrest in DPCs, which was further confirmed by the results that transfection of ocu-miR-205 inhibitor DPCs cells reduced the cell population at G0/G1 phase and increased the apoptotic ratio, and this finding is consistent with previous studies [51]. Further, restored expression of miR-205 significantly inhibited cell proliferation, Besides, ocu-miR-205 inhibitor the expression of related gene and proteins in PI3K/Akt, Wnt, Notch signaling pathway, activation BMP signaling pathway. Therefore, ocu-miR-205 plays an important role in regulating hair follicle development.

Conclusions

ocu-miR-205 could promote the apoptosis of DPCs, inhibit cell proliferation, affect the of PI3K/Akt, Wnt, Notch and BMP signaling pathways genes and proteins expression in DPCs and the skin of Rex rabbits, promote the transformation of hair follicles from growth phase to regression and resting phase, and affect hair density of Rex rabbits.

Abbreviations

BMP: Bone morphogenetic protein; BP: biological process; CC: cellular component; DAG: Directed Acyclic Graph; DEGs: differentially expressed genes screen; DMEM: Dulbecco's modified eagle medium; DMSO: Dimethyl sulfoxide; DP: Dermal papilla; DPCs: Dermal papilla cells; DKK1: Dickkopf relative protein 1; FBS: Fetal bovine serum; FGF: Fibroblast growth factor; GAPDH: Glyceraldehydes-3-phosphate dehydrogenase; GFP: Green flourecent protein; GO: Gene ontology; GSK-3β: Glycogen synthase kinase 3β; HD: High wool density; HE: Hematoxylinand erosin; Lef-1: lymphoid enhancer-binding factor 1; LD: Low wool density; miRNAs: MicroRNAs; mRNA: messenger RNA; MTT: Thiazolyl blue tetrazolium bromide; NOG: Noggin; rRNA: ribosomal RNA; S/P: secondary/primary ratio; snRNA: small nuclear ribonucleic acid; snoRNA: small nucleolar RNA; TGFβ: Transforming growth factor β; TPM: Transcript per million; tRNA: transfer RNA; ocu-miR-205: *Oryctolagus cuniculus* microRNA 205; OD: Optical density; PAGE: polyacrylamide gel electrophoresis; PBS: phosphate buffer saline; PI3K: phosphatidylinositol 3' –kinase.

Declarations

Acknowledgements

We would like to thank our anonymous reviewers and our colleagues from the Animal Nutrition Laboratory for their valuable critiques and suggestions.

Authors' contributions

GL, SL and LB isolation, culture and identification of DPCs, and construction of the small RNA libraries, sequencing analysis, miRNAs identification and prediction of new miRNAs. GL and HS isolated and cultured hair follicles, and performed cellular experiments. GL, HL and SG raised the rabbits and conducted the animal experiments. GL, WJ and FL revised the manuscript. YZ, WJ and FL designed this work and wrote this manuscript.

Funding

This study was supported by the earmarked fund for Modern Agro-industry Technology Research System (CARS-43-B-1), Shandong Natural Science Foundation (ZR2018MC025) and Funds of Shandong “Double Tops” Programme. Construction of the small RNA libraries, sequencing analysis, miRNAs identification and prediction of new miRNAs in DPCs were supported by Modern Agro-industry Technology Research System (CARS-43-B-1), Construction and identification of ocu-miR-205 over expression and interfering expression adenovirus vector were supported by Shandong Natural Science Foundation (ZR2018MC025) and Funds of Shandong “Double Tops” Programme.

Availability of data and materials

The datasets used and/or analysed during the current study are available from the corresponding author on reasonable request.

Ethics approval and consent to participate

The experimental procedures were approved by the Committee of Ethics in Research of Shandong Agricultural University (SDAUA-2017-029) and performed in accordance with the Guidelines for Experimental Animals of the Ministry of Science and Technology (Beijing, China). This article does not any studies with human participants performed by any of the authors.

Consent for publication

Not applicable.

Competing interests

The authors declare that they have no competing interests.

Author details

[1.] College of Animal Science and Technology, Shandong Agricultural University, Tai’an 271018, P. R. China; [2.] Shandong Provincial Key Laboratory of Animal Biotechnology and Disease Control and Prevention, Tai’an 271018, P. R. China; [3.] Animal Husbandry and Veterinary Institute, Shandong Academy of Agricultural Sciences, Jinan 251000, P. R. China [4.] Shandong Key Laboratory of Animal Disease Control and Breeding, Jinan 251000, P. R. China.

References

1. Ruben D. Choosing a Rex rabbit. Small mammal breeds. 2014.

2. Gu Z, Ren W, Huang R, Huang Y, Chen B. Study on density of rex rabbit. Chinese Journal of Rabbit Farming.1999; 4:18-21.

3. Millar SE. Molecular mechanisms regulating hair follicle development. Journal of Investigative Dermatology. 2002; 118:216–225.

4. Fuchs E. Scratching the surface of skin development. Nature. 2007;445:834-842.

5. Lin CM, Yuan Y, Chen X, Li H, Cai B, Liu Y, et al. Expression of Wnt/β–catenin signaling, stem-cell markers and proliferating cell markers in rat whisker hair follicles. Journal of Molecular Histology. 2015;46(3):233-240.

6. Demehri S, Kopan R. Notch signaling in bulge stem cells is not required for selection of hair follicle fate. Development. 2009; 136(6): 891-896.

7. Kulessa H, Turk G, Hogan BL. Inhibition of Bmp signaling affects growth and differentiation in the anagen hair follicle. Embo Journal. 2000;19(24):6664-6674.

8. Su R, Li J, Zhang W, Yin J, Zhao J, Chang Z. Expression of BMP2 in the skin and hair follicle from different stage in Inner Mongolia cashmere goat. Scientia Agricultura Sinica. 2008; 23:559-563.

9. Foitzik K, Lindner G, Mueller-Roever S, Maurer M, Botchkareva N, Botchkarev V, et al. Control of murine hair follicle regression (catagen) by TGF-beta1 in vivo. The FASEB Journal. 2000;14:752-760.

10. Greco V, Chen T, Rendl M, Schober M, Pasolli HA, Stokes N, et al. Two-step mechanism for stem cell activation during hair regeneration. Cell Stem Cell. 2009; 4(2):155–169.

11. Driskell RR, Clavel C, Rendl M, Watt FM. Hair follicle dermal papilla cells at a glance. J. Cell Sci. 2011;124:1179-1182.

12. Chi W, Wu E, Morgan BA. Dermal papilla cell number specifies hair size, shape and cycling and its reduction causes follicular decline. Development. 2013; 140:1676-1683.

13. Woo C, Eleanor W, Bruce A. Morgan permal papilla cell number specifies hair size, shape and cycling and its reduction causes follicular decline. Development and stem cells. 2013; 140: 1676-1683.

14. Yi R, Fuchs E. MicroRNAs and their roles in mammalian stem cells. J. Cell Sci. 2011; 124: 1775–1783.

15. Carrington JC, Ambros V. Role of microRNAs in plant and animal development. Science 2003; 301:336–338.

16. Xu P, Vernooy SY, Guo M, Hay BA. The Drosophila microRNA Mir-14 suppresses cell death and is required for normal fat metabolism. Curr. Biol. 2003; 13: 790–795.

17. Bartel DP. MicroRNAs: genomics, biogenesis, mechanism, and function. Cell 2004; 116:281–297.

18. Teleman AA., Maitra S, Cohen SM. Drosophila lacking microRNA miR-278 are defective in energy homeostasis. Genes Dev. 2006; 20: 417–422.

19. He L, Lim LP, Stanchina E, Xuan Z, Liang Y, Xue W, et al. A microRNA component of the p53 tumour suppressor network. Nature. 2007; 447:1130–1134.

20. Mardaryev AN, Ahmed MI, Vlahov NV, Fessing MY, Gill J H, Sharov AA, et al. Micro-RNA-31 controls hair cycle-associated changes in gene expression programs of the skin and hair follicle. FASEB Journal. 2010; 24 (10), 3869 -3881.

21. Liu Z, Xiao H, Li H, Zhao Y, Lai S, Yu X, et al. Identification of conserved and novel microRNAs in cashmere goat skin by deep sequencing. Plos One. 2012; 7(12): 50001.

22. Wang P, Hong W, Zhen J, Ren J, Li Z, Xu A. The changes of microRNA expression profles and tyrosinase related proteins in MITF knocked down melanocytes. Molecular BioSystems. 2012; 8: 2924-2931.

23. Ahmed MI, Alam M, Emelianov VU. MicroRNA214 controls skin and hair follicle development by modulating the activity of the Wnt pathway. Journal of Cell Biology. 2014; 207(4), 549-567.

24. Andl T, Murchison EP, Liu F, Zhang Y, Yunta-Gonzalez M, Tobias JW, et al. The miRNA-processing enzyme dicer is essential for the morphogenesis and maintenance of hair follicles. Current Biology. 2006;16(10), 1041–1049.

25. Shen Y, Zhang Y, Liu N, Wang H, Xie J, Gao S, et al. Let-7b promotes alpaca hair growth via transcriptional repression of TGFβRI. Gene. 2016; 577:32–36.

26. Ahmed MI, Mardaryev AN, Lewis CJ, Sharov AA, Botchkareva NV. MicroRNA-21 is an important downstream component of BMP signaling in epidermal keratinocytes. Journal of Cell Science 2011; 124(20), 3399–3404.

27. Gregory PA, Bert AG, Paterson EL, Barry SC, Tsykin A, Farshid G, et al. The miR-200 family and miR-205 regulate epithelial to mesenchymal transition by targeting ZEB1 and SIP1. Nat. Cell Biol. 2008; 10, 593–601.

28. Yi R, O\"Carroll D, Hilda AZ, Zhihong D, Fred ST, Alexander F, et al. Morphogenesis in skin is governed by discrete sets of differentially expressed microRNAs. Nat. Genet. 2006; 38, 356–362.

29. Ryan DG, Oliveira-Fernandes M, Lavker RM. MicroRNAs of the mammalian eye display distinct and overlapping tissue specificity. Mol. Vis. 2006; 12, 1175–1184.

30. Wang D, Zhang Z, O'Loughlin E, Wang L, Fan X, Lai E. et al. MicroRNA-205 controls neonatal expansion of skin stem cells by modulating the PI(3)K pathway. Nat. Cell Biol. 2013;15, 1153–1163.

31. Wu M, Sun Q, Guo X, Liu H. hMSCs possess the potential to differentiate intoc DP cells in vivo and in vitro. Cell Biol. Int. Rep. 2010; 19 (2), e00019.

32. Lim LP, Glasner ME, Yekta S, Burge CB, Bartel DP. Vertebrate microRNA genes. Science. 2003; 299, 1540.

33. Wienholds E, Plasterk RH. MicroRNA function in animal development. FEBS Lett. 2005; 579, 5911–5922.

34. Du T, Zamore PD. Beginning to understand microRNA function. Cell Res. 2007; 17:661–663.

35. Kollar EJ. The induction of hair follicles by embryonic dermal papillae. J. Invest. Dermatol. 1970; 55:374-378.

36. Oliver RF. The induction of hair follicle formation in the adult hooded rat by vibrissa dermal papillae. J. Embryol. Exp. Morphol. 1970; 23:219-236.

37. Jahoda CA, Horne KA, Oliver RF. Induction of hair growth by implantation of cultured dermal papilla cells. Nature1984; 311:560-562.

38. Yi R., O\"Carroll D, Hilda AZ, Zhihong D, Fred ST, Alexander F, et al. Morphogenesis in skin is governed by discrete sets of differentially expressed microRNAs. Nat. Genet. 2006; 38:356–362.

39. Ryan DG, Oliveira-Fernandes M, Lavker RM. MicroRNAs of the mammalian eye display distinct and overlapping tissue specificity. Mol. Vis. 2006; 12: 1175–1184.

40. Wang D, Li Q, Feng N, Cheng G, Guan Z, Wang Y, et al. MicroRNA-205 controls neonatal expansion of skin stem cells by modulating the PI3K pathway. Nat. Cell Biol., 2013; 15:1153–1163.

41. Yu J, Peng H, Ruan Q, Fatima A, Getsios S, Lavker RM, et al. MicroRNA-205 promotes keratinocyte migration via the lipid phosphatase SHIP2. FASEB J. 2010; 24:3950–3959.

42. Lin D, Halilovic A, Yue P, Bellner L, Wang K, Wang L, et al. Inhibition of miR-205 impairs the wound-healing process in human corneal epithelial cells by targeting KIR4.1 (KCNJ10). Invest. Ophthalmol. Vis. Sci. 2013; 54:6167–6178.

43. Xie H, Zhao Y, Caramuta S, Larsson C, Lui WO. miR-205 expression promotes cell proliferation and migration of human cervical cancer cells. PLoS One. 2012; 7:e46990.

44. Li C, Finkelstein D, Sherr C. J. Arf tumor suppressor and miR-205 regulate cell adhesion and formation of extraembryonic endoderm from pluripotent stem cells. Proc. Natl. Acad. Sci. U. S. A. 2013; 110:E1112–E1121.

45. Tucci P, Agostiniet M, Grespi F, Markert E, Terrinoni A, Vousden K, et al. Loss of p63 and its microRNA-205 target results in enhanced cell migration and metastasis in prostate cancer. Proc. Natl. Acad. Sci. U. S. A. 2012; 109: 15312–15317.

46. Liu S, Tetzlaff M, Liu A, Liegl-Atzwanger B, Guo J, Xu X. Loss of microRNA-205 expression is associated with melanoma progression. Lab. Investig. 2012; 92:1084–1096.

47. Majid S, Saini S, Dar A, Hirata H, Shahryari V, Tanaka Y, et al. MicroRNA-205 inhibits Src-mediated oncogenic pathways in renal cancer. Cancer Res. 2011; 71:2611–2621.

48. Gandellini P, Folini M, Longoni N, Pennati M, Binda M, Colecchia M, et al. miR-205 exerts tumor-suppressive functions in human prostate through down-regulation of protein kinase Cepsilon. Cancer Res. 2009;69:2287–2295.

49. Larzabal L, Redrado M, Aberasturi A, Rueda P, Rodríguez M, Lopez L, et al. TMPRSS4 regulates levels of integrin α5 in NSCLC through miR-205 activity to promote metastasis. British Journal of Cancer, 2014;110:764–774.

50. Wang N, Li Q, Feng N, Cheng G, Guan Z, Wang Y, et al. miR-205 is frequently downregulated in prostate cancer and acts as a tumor suppressor by inhibiting tumor growth. Asian J. Androl. 2013;15:735–741.

51. Zhang J, He X, Tong W, Johnson T, Wiedemann L, Mishina Y, et al. Bone morphogenetic protein signaling inhibits hair follicle anagen induction by restricting epithelial stem/progenitor cell activation and expansion. Stem Cells 2006; 24:2826-2839.

52. Zhang H, Wang S, Zhang T, Si H, Wang D, Yang F, et al. Epidermal growth factor promotes proliferation of dermal papilla cells via Notch signaling pathway. Biochimie 2016; 127:10-18.

53. Wang Z, Gerstein M, Snyder M. RNA-Seq: a revolutionary tool for Transcriptomics. Nature Reviews Genetics. 2009; 10(1):57-63.

54. Mortazavi A, Williams BA, McCue K, Schaeffer L. Mapping and quantifying mammalian transcriptomes by RNA-Seq. Nature Methods. 2008;5(7): 621-628.

55. Eric PN, Sarah WB, Alex B, Jennifer D, Ruth YE, Sean RE, et al. Rfam 12.0: updates to the RNA families database. Nucleic Acids Research. 2014;43: D130-137.

56. Kozomara A, Griffiths-Jones S. miRBase: annotating high confidence microRNAs using deep sequencing data. NAR. 2014;42: D68-D73.

57. Friedlander MR, Chen W, Adamidic C, Maaskoia J, Einspanier R, Knespel S, et al. Discovering microRNAs from deep sequencing data using miRDeep. Nature Biotechnology 2008;26:407-415.

58. Peter AC, Yavuz A, Heleneb HT, Erno V, Rolf H, Renée X, Judith M, et al. Deep sequencing-based expression analysis shows major advances in robustness, resolution and inter-lab portability over five microarray platforms. Nucleic Acids Res. 2008;36(21): e141.

59. Jiang H, Wong WH. Statistical inferences for isoform expression in RNASeq. Bioinformatics 2009;25:1026-1032.

60. Yang YH, Dudoit S, Luu P, Lin DM, Peng V, Ngai J. Normalization for cDNA microarray data: a robust composite method addressing single and multiple slide systematic variation. Nucleic Acids Res. 2002;30: e15.

61. Wang L, Feng Z, Wang X, Wang X, Zhang X. DEGseq: an R package for identifying differentially expressed genes from RNA-seq data. Bioinformatics. 2010;26(1):136-138.

62. John B, Enright AJ, Aravin AA, Tuschl T, Sander C, Marks DS. Human MicroRNA targets. Plos. Biology. 2005;3(7), e264.

63. Kanehisa M, Araki M, Goto S, Hattori M, Hirakawa M, Itoh M, et al. KEGG for linking genomes to life and the environment. Nucleic Acids Res. 2008;36: D480-484.

64. Ouji Y, Yoshikawa M, Moriya K, Ishizaka S. Effects of Wnt-10b on hair shaft growth in hair follicle cultures. Biochem. Biophys. Res. Commun. 2007;359:516–522.

65. LiLivak KJ, Schmittgen TD. Analysis of relative gene expression data using real-time quantitative PCR and the $2^{-\Delta\Delta CT}$ method. Methods. 2001; 25: 402–408.

Tables

Table 1. Effects of ocu-miR-205 on proliferation, cell cycle and apoptosis of dermal papilla cells (DPCs; %)

Items	Group				R-MSE	*P*-value
	Control	HBAD-GFP	HBAD-ocu-miR-205-GFP	HBAD-ocu-miR-205-5p-sponge-GFP		
Proliferation of dermal papilla cells						
Optical density (OD) value	0.56±0.01^{b}	0.55±0.01^{b}	0.61±0.01^{a}	0.34±0.01^{c}	0.0356	<0.0001
Cell cycle of dermal papilla cells						
Resting state/first gap (G0/G1)	87.79±1.00^{a}	84.68±1.01^{b}	77.71±0.88^{c}	85.57±1.03^{ab}	2.7795	<0.0001
Synthesis (S)	7.15±0.85^{b}	9.48±0.95^{b}	14.73±0.62^{a}	8.97±0.68^{b}	2.2232	<0.0001
Second gap/mitosis (G2/M)	5.07±0.24^{b}	5.37±0.49^{b}	7.56±0.37^{a}	5.46±0.35^{b}	1.0523	0.0002
Apoptosis of dermal papilla cells						
Early apoptotic ratio (Q4)	33.95±0.40^{b}	32.86±1.04^{b}	36.71±0.67^{a}	29.16±0.47^{c}	1.9470	<0.0001
Later apoptotic ratio (Q2)	33.46±0.57^{b}	32.15±1.33^{b}	36.11±0.73^{a}	31.40±0.57^{b}	2.4323	0.0032
Total apoptosis ratio (Q4+Q2)	67.41±0.51^{b}	65.01±1.50^{b}	72.83±1.14^{a}	60.56±0.47^{b}	2.8310	<0.0001

Note: Data shown are mean values ± s. d., and n = 8 per group. In the same row, values with same letter superscripts mean no significant difference (P>0.05), with different letter superscripts mean significant difference (P<0.05).

Table 2. Effects of ocu-miR-205 on gene expression of signal pathway of dermal papilla cells (DPCs)

Gene	Group				R-MSE	*P*-value
	Control	HBAD-GFP	HBAD-ocu-miR-205-GFP	HBAD-ocu-miR-205-5p-sponge-GFP		
PI3K/Akt signal pathway						
Inppl1	1.00±0.09^{b}	1.02±0.04^{b}	0.80±0.07^{b}	1.68±0.12^{a}	0.2353	<0.0001
Inpp4b	1.00± 0.09	0.97±0.16	0.92±0.08	1.21±0.16	0.3598	0.3966
Frk	1.00±0.34^{b}	0.90±0.07^{b}	0.50±0.13^{c}	2.63±0.47^{a}	0.8442	0.0001
Phlda3	1.00± 0.04^{b}	0.89±0.06^{b}	0.69±0.05^{c}	1.18±0.05^{a}	0.1491	<0.0001
Wnt signal pathway						
Wnt10b	1.00±0.11^{b}	0.95±0.09^{b}	0.38±0.11^{c}	2.24±0.17^{a}	0.3519	<0.0001
CTNNB1	1.00±0.09^{b}	1.50±0.13^{b}	1.48±0.19^{b}	3.16±0.27^{a}	0.5186	<0.0001
GSK-3β	1.00± 0.14^{b}	0.97±0.05^{b}	2.66±0.68^{a}	3.22±0.71^{a}	1.4118	0.0050
DKK1	1.00±0.09^{c}	2.90±0.13^{b}	6.09±0.84^{a}	0.84±0.07^{c}	1.2141	<0.0001
Notch signal pathway						
Notch1	1.00±0.08^{b}	0.96±0.07^{b}	0.39±0.02^{c}	1.19±0.03^{a}	0.1604	<0.0001
Jagged1	1.00±0.07^{ab}	0.81±0.13^{bc}	0.60±0.10^{c}	1.12±0.07^{a}	0.2679	0.0032
Hes1	1.00±0.12^{b}	1.19±0.16^{b}	0.90±0.05^{b}	2.40±0.33^{a}	0.5475	<0.0001
Hes5	1.00± 0.16^{b}	1.04±0.06^{b}	0.18±0.04^{c}	1.38±0.04^{a}	0.2477	<0.0001
BMP signal pathway						
BMP2	1.00±0.15^{b}	0.51±0.05^{bc}	1.69±0.34^{a}	0.41±0.05^{c}	0.5408	0.0002
BMP4	1.00± 0.20^{ab}	1.11±0.18^{ab}	1.34±0.08^{a}	0.63±0.13^{b}	0.4405	0.0254
TGF-β1	1.00±0.05^{ab}	0.89±0.18^{b}	1.33±0.13^{a}	0.71±0.07^{b}	0.3304	0.0071

Note: Data shown are mean values ± s. d., and n = 8 per group. In the same row, values with no letter superscripts or same letter superscripts mean no significant difference (*P*>0.05), with different letter superscripts mean significant difference(*P*<0.05).

Table 3. Effects of ocu-miR-205 on gene expression of signal pathway of Rex rabbits skin

Gene	Group				R-MSE	*P*-value
	Control	HBAD-GFP	HBAD-ocu-miR-205-GFP	HBAD-ocu-miR-205-5p-sponge-GFP		
PI3K/Akt signal pathway						
Inppl1	1.00±0.09^{b}	0.99±0.07^{b}	0.54±0.03^{c}	2.30±0.15^{a}	0.2731	<0.0001
Inpp4b	1.00± 0.15^{ab}	0.89± 0.07^{a}	0.09±0.01^{b}	1.05±0.02^{a}	0.2348	<0.0001
Frk	1.00±0.26^{a}	1.16±0.05^{b}	0.31±0.02^{c}	1.94±0.20^{a}	0.4666	<0.0001
Phlda3	1.00± 0.11^{b}	1.18± 0.11^{a}	0.27±0.03^{b}	1.18±0.11^{a}	0.2500	<0.0001
Wnt signal pathway						
Wnt10b	1.00±0.14^{b}	0.86±0.04^{bc}	0.74±0.04^{c}	1.26±0.09^{a}	0.2406	0.0011
CTNNB1	1.00±0.07^{b}	0.98±0.05^{b}	0.75±0.04^{c}	1.30±0.08^{a}	0.1789	<0.0001
GSK-3β	1.00± 0.06^{ba}	1.04±0.07^{b}	0.85±0.04^{b}	1.10±0.05^{a}	0.1496	0.0198
DKK1	1.00±0.36^{a}	0.91±0.10^{a}	1.28±0.10^{a}	0.18±0.07^{b}	0.5625	0.0041
Notch signal pathway						
Notch1	1.00±0.18^{b}	0.83±0.05^{bc}	0.54±0.05^{c}	1.95±0.22^{a}	0.4131	<0.0001
Jagged1	1.00±0.13^{a}	1.02±0.05 ^{a}	0.36±0.03^{c}	1.34±0.22 ^{a}	0.3670	0.0001
Hes1	1.00±0.09^{b}	1.03±0.06^{b}	0.80±0.03^{b}	1.49±0.18^{a}	0.3042	0.0009
Hes5	1.00± 0.13 ^{b}	1.00±0.05^{b}	0.36±0.03^{c}	1.43±0.20^{a}	0.3435	<0.0001
BMP signal pathway						
BMP2	1.00±0.15^{b}	1.02±0.07^{b}	1.39±0.08^{a}	0.64±0.10^{c}	0.3051	0.0005
BMP4	1.00± 0.15^{b}	0.87±0.04^{b}	1.58±0.14^{a}	0.73±0.05^{b}	0.3081	<0.0001
TGF-β1	1.00±0.12 ^{ab}	0.88±0.05 ^{bc}	1.15±0.06^{a}	0.67±0.05^{b}	0.2222	0.0014

Note: Data shown are mean values ± s. d., and n = 8 per group. In the same row, values with same letter superscripts mean no significant difference (P>0.05), with different letter superscripts mean significant difference (P<0.05).

Table 4. Effects of ocu-miR-205 on hair follicle density of Rex rabbits (Count/mm^2)

Items	Group				R-MSE	*P*-value
	Control	HBAD-GFP	HBAD-ocu-miR-205-GFP	HBAD-ocu-miR-205-5p-sponge-GFP		
Transfection for 7 days						
Hair follicle density	125.57±9.63^{bc}	144.25±11.47^{ba}	105.02±5.89^{c}	163.94±16.68^{a}	32.7817	0.0085
Primary hair follicle density	10.08±0.85	9.31±0.85	7.80±0.63	9.79±0.77	2.2046	0.1902
Secondary hair follicle density	115.49±9.48^{bc}	134.93±12.01^{ba}	97.22±5.68^{c}	154.15±16.65^{a}	32.9728	0.0113
Secondary/Primary (S/P) ratio	11.92±1.17	16.02±2.67	12.92±1.06	16.38±2.04	5.2469	0.2536
Transfection for 14 days						
Hair follicle density	130.54±12.22^{b}	136.62±8.51^{b}	119.30±7.24^{b}	203.34±14.79^{a}	31.4005	<0.0001
Primary hair follicle density	10.86±0.54	9.96±0.50	11.92±0.74	10.11±0.70	1.7739	0.1307
Secondary hair follicle density	119.68±12.03^{b}	126.66±8.28^{b}	107.37±7.10^{b}	213.32±14.62^{a}	30.9035	0.0001
Secondary/Primary (S/P) ratio	11.08±0.96 ^{b}	12.82±0.82 ^{b}	9.20±0.78 ^{b}	21.62±1.94 ^{a}	3.4505	<0.0001
Transfection for 21 days						
Hair follicle density	145.43±13.71^{b}	139.58±16.53^{b}	126.38±9.30^{b}	208.69±21.42^{a}	44.8651	0.0049
Primary hair follicle density	14.30±1.19	12.65±0.80	12.92±0.51	15.29±1.28	2.8084	0.2244
Secondary hair follicle density	131.13±13.21^{b}	126.94±16.57^{b}	113.46±9.27^{b}	193.40±21.31^{a}	44.4697	0.0060
Secondary/Primary (S/P) ratio	9.45±0.91	10.28±1.40	8.86±0.75	13.28±1.85	3.6808	0.1018

Note: Data shown are mean values ± s. d., and n = 8 per group. In the same row, values with no letter superscripts or same letter superscripts mean no significant difference (P>0.05), with different letter superscripts mean significant difference (P<0.05).

Figures

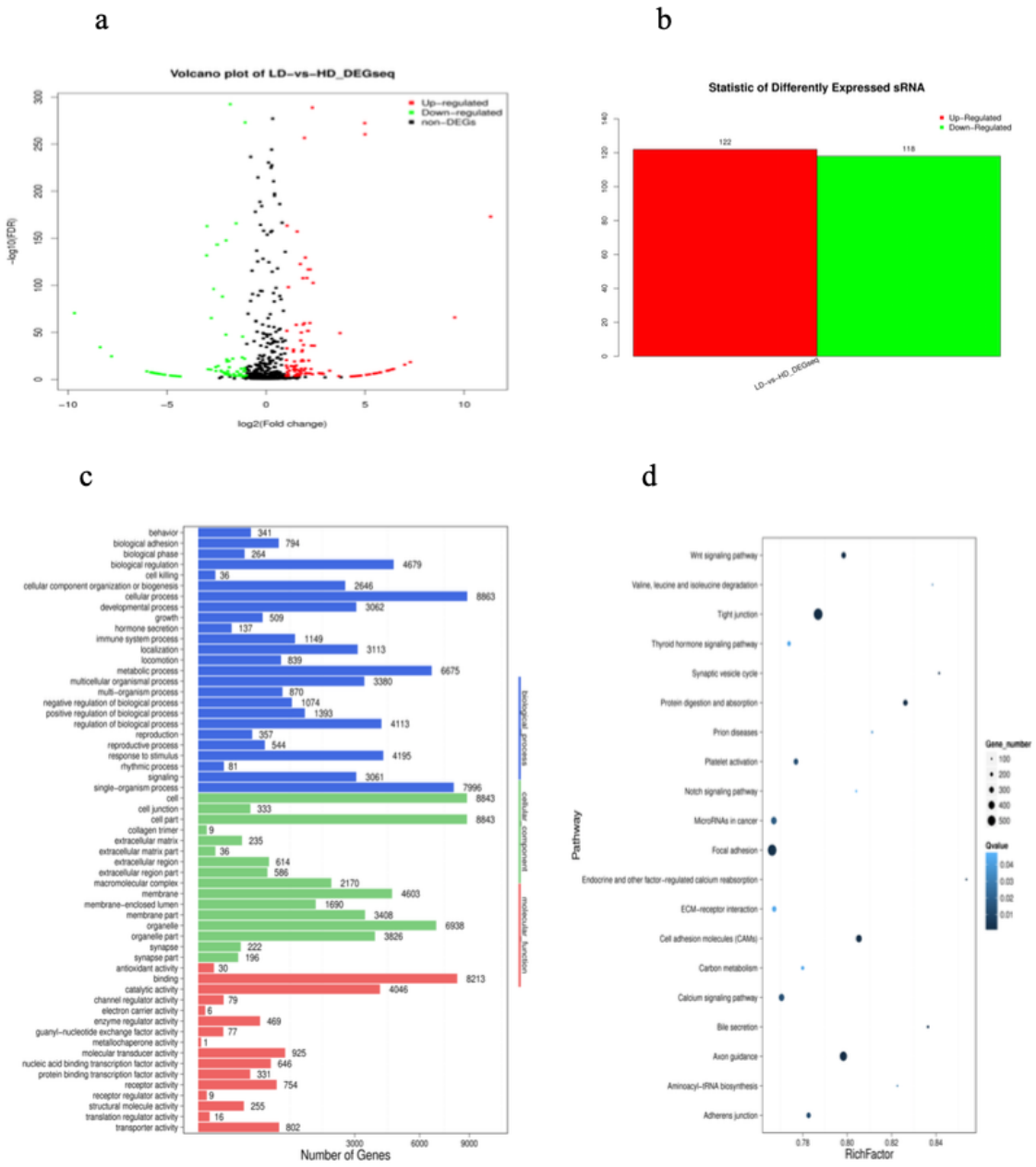

Figure 1

Differentially expressed miRNAs (a) Differential miRNAs volcanic map; (b) Significantly differential expressed miRNAs; (c) GO functional classification of differential miRNA target genes; (d) Pathway enrichment statistical scatter plot

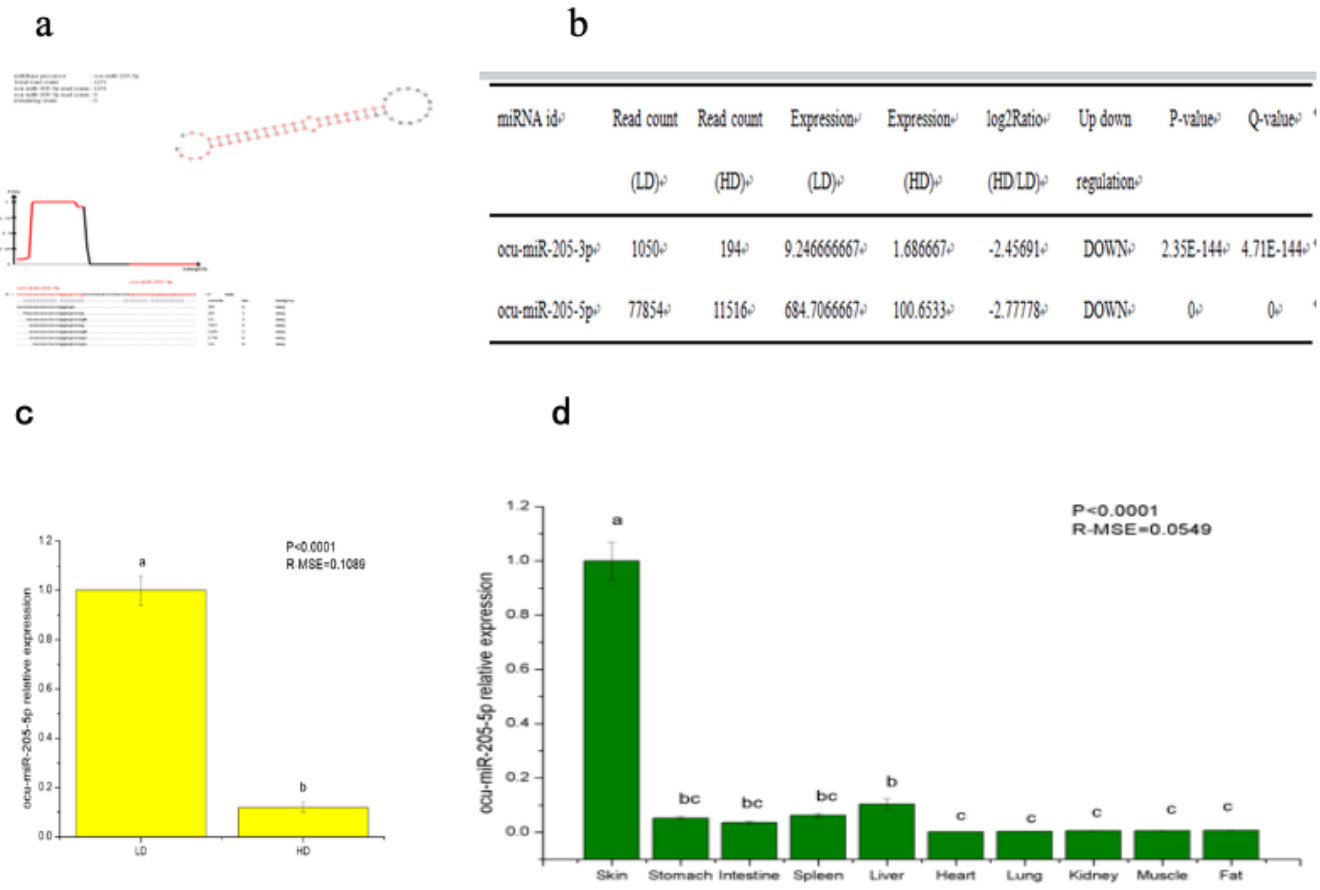

Figure 2

Expression of ocu-miR-205-5p (a) Structure of ocu-miR-205; (b) Expression of ocu-miR-205 in dermal dermal papilla cells of rabbits with different density density detected by high-throughput sequencing; (c) Real-time PCR analysis of ocu-miR-205-5p expression in dermal papilla cells with different wool density. Mean values ± s.d., n =3, a,b mean P< 0.05. (d) Real-time PCR analysis of ocu-miR-205-5p expression in different tissues of Rex rabbits, Mean values ± s.d., n=8, a,b mean P< 0.05. Rex raabbits were 30 days old, four for male, four for female.

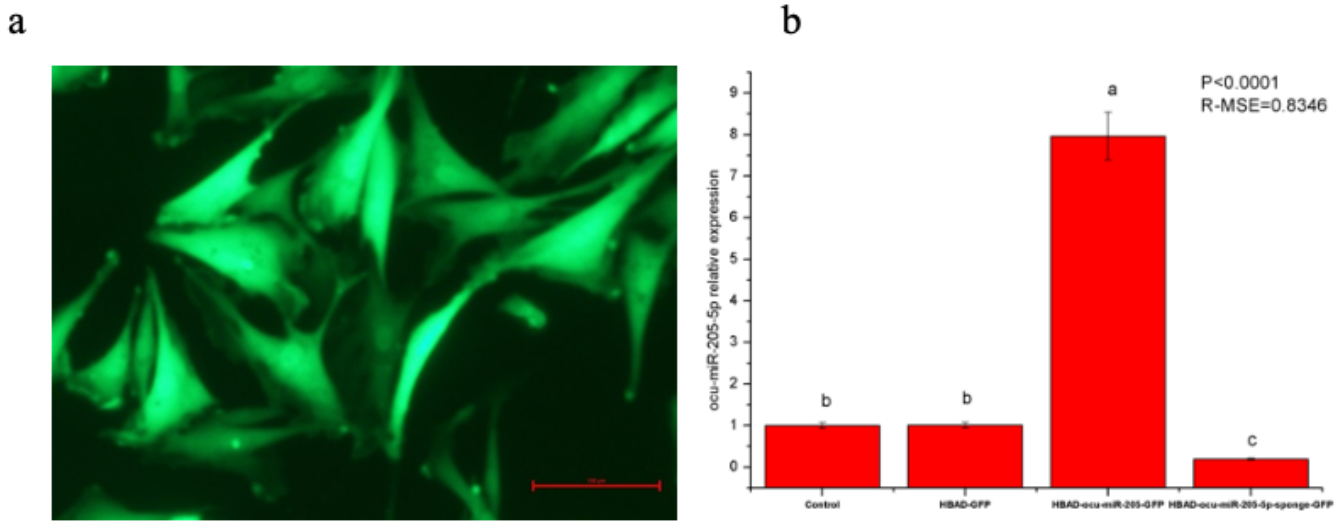

Figure 3

Effects of adenovirus transfection on dermal papilla cells (a) Transfection 24h, fluorescence microscope (200 magnification); (b) Expression of ocu-miR-205-5p in dermal papilla cells after transfection 48 h detected by quantitative fluorescence quantification, Mean values ± s.d., a,b mean P< 0.05, n=8.

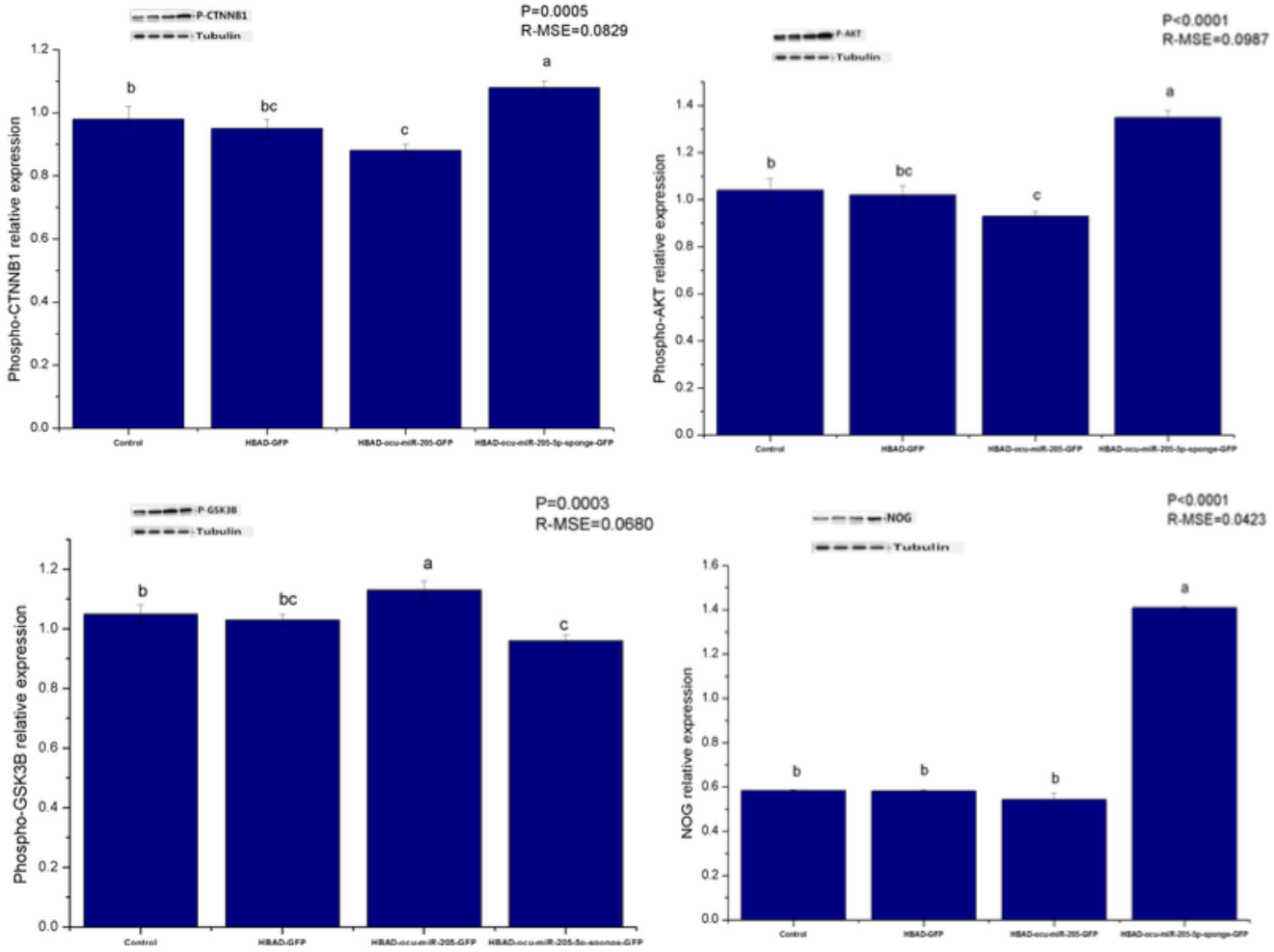

Figure 4

Effects of ocu-miR-205 on expression of hair follicle-related proteins of dermal papilla cells Mean values ±s.d., and n = 8 per group. In the same graph, values with same letter superscripts mean no significant difference (P>0.05), with different letter superscripts mean significant difference (P<0.05).

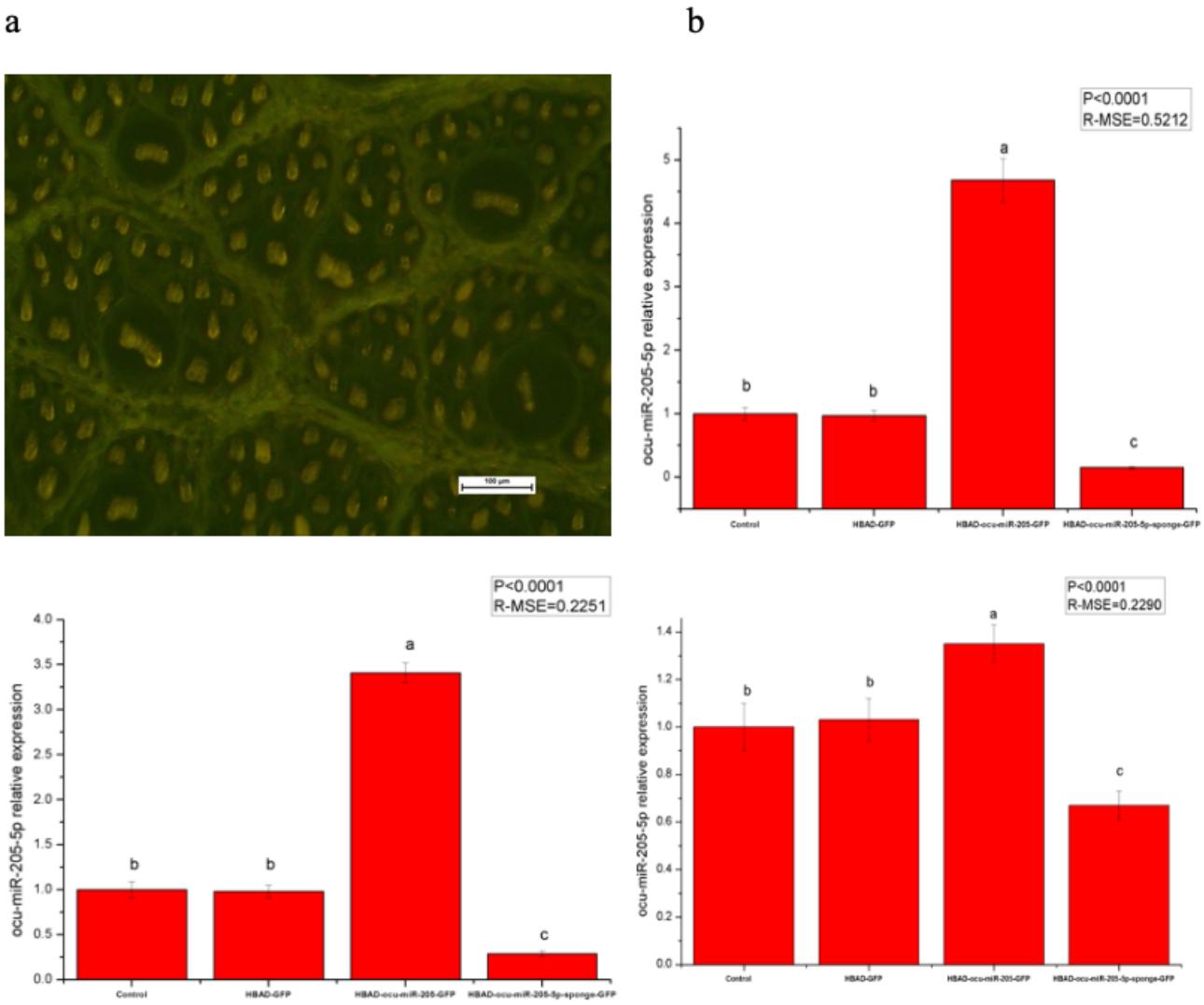

Figure 5

Effects of adenovirus transfection on skin follicles of Rex rabbits (a) Frozen slice crosscutting of Rex rabbits skin (200 magnification); (b) Expression of ocu-miR-205-5p in dermal papilla cells after transfection 7d, 14d, 21d detected by quantitative fluorescence quantification, Mean values ±s.d., a,b mean P< 0.05, n=8.

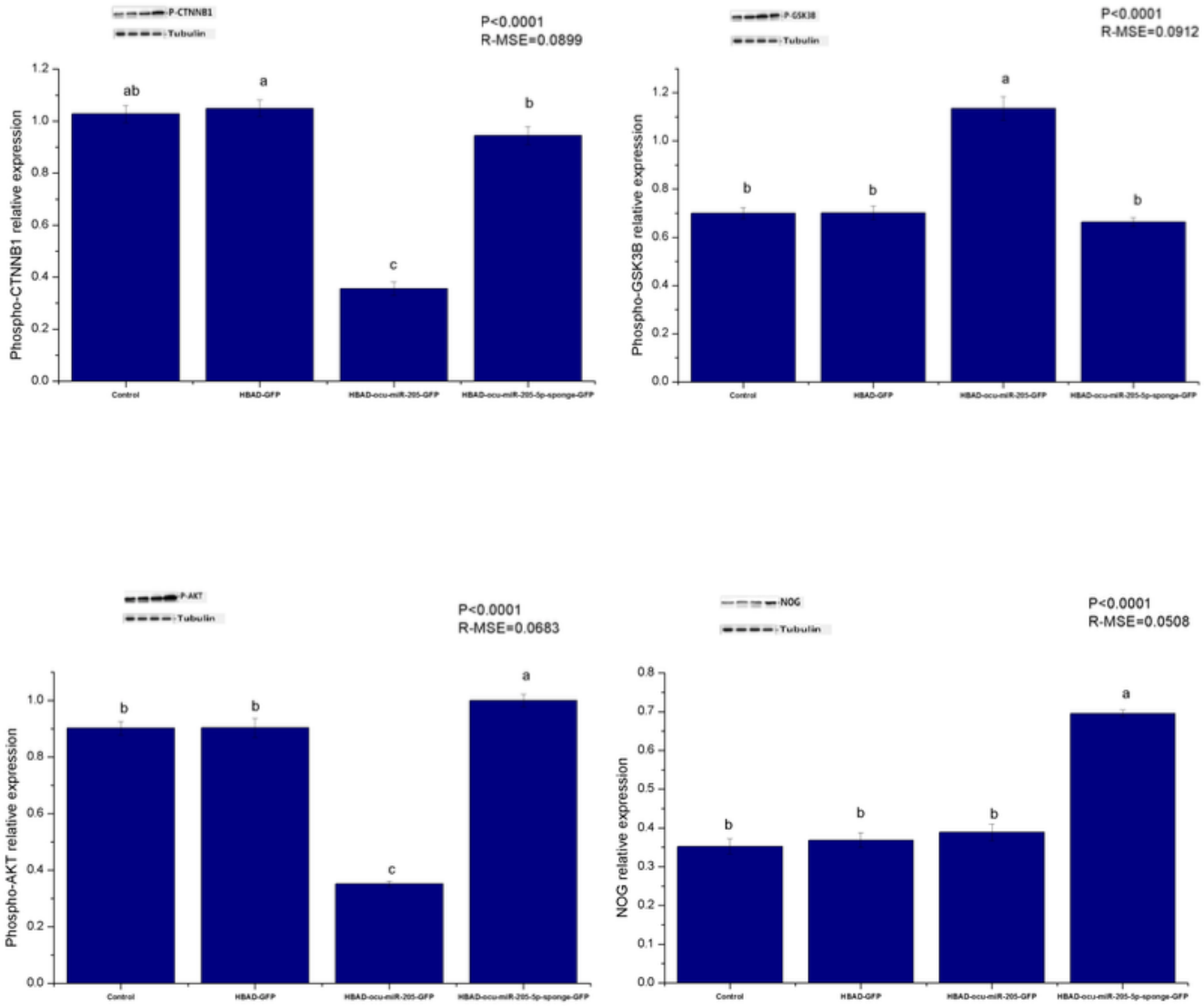

Figure 6

Effects of ocu-miR-205 on expression of hair follicle-related proteins of Rex rabbits skin Mean values ± s.d., and n = 8 per group. In the same graph, values with same letter superscripts mean no significant difference (P>0.05), with different letter superscripts mean significant difference (P<0.05).

Supplementary Files

This is a list of supplementary files associated with this preprint. Click to download.

- supplement1.docx
- supplement2.docx
- supplement3.docx
- supplement4.docx